Jurnal Fisika Unand (JFU)
Vol. 15, No. 4, Juli 2026, hal. 363 – 371
ISSN: 2302-8491 (Print); 2686-2433 (Online)
https://doi.org/10.25077/jfu.15.4.363-371.2026

Open Access

Identification of Weak Zones with Resistivity Values Using Electrical Resistivity Imaging in Bentiring Subdistrict, Bengkulu

Adrian Daniel, Halauddin*, Suhendra, Muhammad Taufik Apriadi, Agung Wijaya, Lulu Indah Setyawati, Hana Raihana
[1]Department of Geophysics, Faculty of Mathematics and Natural Sciences, the University of Bengkulu

Article Info

Article History:
Submitted: 15 January 2026
Revised: 20 March 2026
Accepted: 31 July 2026

Keywords:
Bentiring
ERI
Weak Zone
Wenner-Schlumberger

Corresponding Author:
Halauddin
Email: halaukualasatu@gmail.com

ABSTRACT

Bentiring Subdistrict Bentiring Subdistrict is an area composed of alluvial deposits with a shallow water table, a condition often associated with road damage and building subsidence. These conditions indicate the presence of subsurface weak zones that have the potential to cause soil instability; therefore, geophysical investigations are required to map these zones as a basis for geotechnical hazard mitigation. This study aims to identify subsurface weak zones using the Electrical Resistivity Imaging (ERI) method with a Wenner–Schlumberger configuration. Data processing involved field data correction, filtering to reduce noise, and 2D inversion to generate a subsurface resistivity distribution model. The inversion results show a low-resistivity zone ranging from 8.78 to 28.2 Ω·m, interpreted as clay to silty sandstone with high water content. This zone is consistently detected across all survey lines and is particularly prominent in the middle to lower parts of the section, at depths of approximately 2.7–78.8 m. The consistency of the lateral distribution indicates that this weak zone is continuous beneath the study area. The presence of this water-saturated layer with low resistivity indicates soft and easily deformable material, which has the potential to contribute to ground subsidence and surface deformation occurring in the study area. The results of this study demonstrate that the ERI method is effective in identifying and mapping weak zones in alluvial environments, and provides important geophysical information to support spatial planning and geotechnical risk mitigation in Bentiring Subdistrict.

Copyright © 2026 Author(s).

I. INTRODUCTION

Ground instability and subsurface weakening represent important geotechnical and environmental concerns because variations in lithology, structural conditions, and groundwater distribution may reduce the mechanical strength of near-surface materials and affect surface infrastructure. In many regions of Indonesia, phenomena such as ground cracking, differential settlement, and localized ground deformation are often associated with heterogeneous subsurface conditions. Understanding the distribution of subsurface materials therefore becomes essential for identifying zones that potentially exhibit lower mechanical competence. Geoelectric methods have been widely applied to investigate subsurface conditions through variations in electrical resistivity associated with lithology, porosity and water saturation. One frequently used configuration is the Wenner-Schlumberger configuration, as it offers good sensitivity to both lateral and vertical variations in resistivity and is capable of providing a reasonably optimal depth of penetration. This configuration also has a good signal-to-noise ratio, making it effective for use in areas with heterogeneous subsurface conditions. For example, geophysical investigations into road pavement damage in south-western Nigeria have shown that variations in subsurface materials, such as weathered layers and clay-rich zones, significantly affect soil stability and structural performance (Adenika et al., 2018). The Wenner–Schlumberger array was selected because it has good sensitivity to both vertical and lateral resistivity variations, making it suitable for identifying subsurface heterogeneity related to weak zones.

In Indonesia, several studies have used geoelectrical approaches to identify weak zones associated with ground instability. A resistivity study along the Samarinda–Bontang roadway indicated that low-resistivity zones correspond to clay-rich and water-saturated materials that may reduce the bearing capacity of the ground (Fatoni et al., 2021). Similarly, research in Banyumas demonstrated that subsurface layers dominated by clay and saturated sediments can be identified as weak zones that potentially contribute to ground subsidence (Makmur et al., 2016). In landslide-prone areas, resistivity contrasts have also been used to delineate zones composed of weathered and saturated materials with relatively low mechanical strength (Wulandari et al., 2024). Geoelectrical investigations have also been widely applied for structural and hydrogeological studies. Resistivity discontinuities have been interpreted as indicators of subsurface fault structures or fractured zones that may influence ground stability (Lutfinur et al., 2015; Pesma & Sitanggang, 2024). In addition, groundwater investigations in pyroclastic deposits demonstrate that the presence of water significantly affects resistivity distribution, particularly in porous and clay-rich materials (Paembonan et al., 2020).

Local studies in Bengkulu using vertical electrical sounding also indicate that variations in subsurface resistivity are closely related to lithological differences and groundwater conditions (Nuraini, 2023). A geoelectrical investigation in the Ponjong area, Gunung Kidul, also showed that resistivity variations can be used to characterize subsurface lithology and identify zones dominated by soft and weathered materials that are considered susceptible to ground instability (Rizqi et al., 2020). These studies confirm that geoelectrical methods are effective for imaging subsurface resistivity variations and identifying lithological contrasts. However, most previous studies primarily focus on identifying subsurface materials or structural features based on resistivity contrasts without explicitly discussing the limitations of resistivity data in explaining deformation processes. Electrical resistivity measurements represent variations in the electrical properties of subsurface materials and do not directly measure mechanical deformation, vertical ground displacement, or land subsidence. Therefore, interpretations derived from Electrical Resistivity Imaging (ERI) should not be considered as direct evidence of deformation processes, but rather as indicators of subsurface heterogeneity that may influence ground stability. Variations in resistivity values commonly reflect differences in lithology, porosity, water saturation, weathering degree, and the presence of weak or unconsolidated materials.

Based on these considerations, this study aims to analyze the distribution of subsurface resistivity using the ERI method to identify potential weak zones associated with ground instability within the study area. The ERI method provides two-dimensional resistivity imaging that enables clearer identification of lateral and vertical variations in subsurface materials compared to conventional sounding approaches. In this context, zones characterized by low resistivity values are interpreted as areas containing weak, weathered, water-saturated, or clay-rich materials that may reduce subsurface stability. Thus, the interpretation presented in this study is limited to geological indications of potential

ground instability inferred from resistivity contrasts and subsurface heterogeneity, rather than direct evidence of land subsidence or measurable surface deformation.

II. METHOD

2.1 Regional Geology

The study area in Bengkulu City is situated within a tectonically active region influenced by the Sumatra Fault system (Lubis et al., 2019). Nevertheless, this study emphasizes shallow geological conditions that control near-surface resistivity distribution and the formation of weak zones. Geoelectrical methods are widely applied to detect subsurface structural contrasts and fault-related weak zones based on resistivity variations (Manuho et al., 2015). The local geology is dominated by Quaternary alluvial deposits and the Bintunan Formation (Sugianto et al., 2016). These alluvial deposits consisting of gravel, sand, fine silt and unconsolidated clay with varying grain sizes and moisture content. These materials are generally loose, porous and locally water-saturated, resulting in relatively low resistivity values, particularly in clay-rich layers. Variations in lithology, moisture content, compaction, and weathering within the alluvial deposits produce distinct resistivity contrasts that can be detected using the Electrical Resistivity Imaging (ERI) method. These contrasts may indicate the presence of mechanically weak zones in the shallow subsurface environment associated with reduced soil stability.

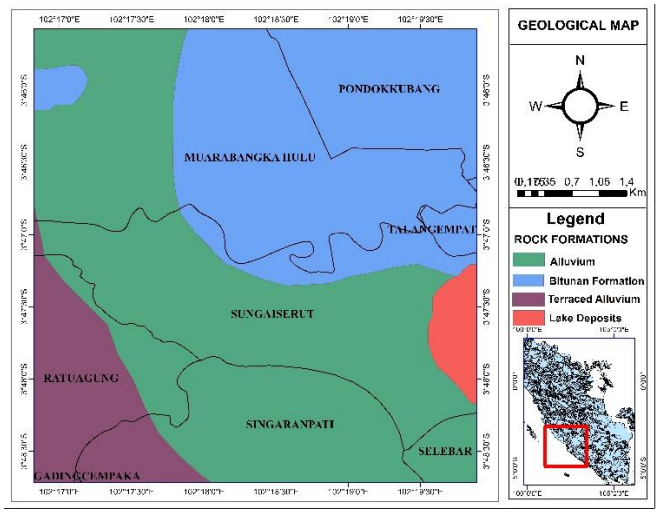


Figure 1. Geological map of Bengkulu City (Gafoer et al., 2007)

2.2 Methodology

This research was conducted from October to November 2024 in the Bentiring Subdistrict, Muara Bangkahulu District, Bengkulu City. Two-dimensional geoelectric data were collected along five survey lines, while data processing was carried out at the Geophysics Laboratory, Faculty of Mathematics and Natural Sciences, Bengkulu University. The research location is shown in Figure 2.

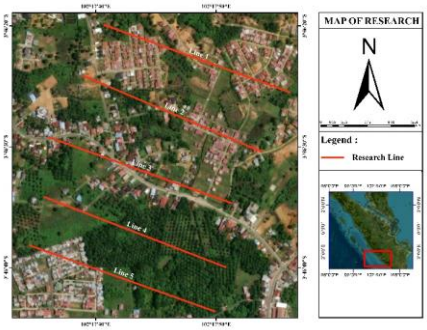


Figure 2. Research location map

This study applied the Electrical Resistivity Imaging (ERI) method using MAE X612EM multichannel geophysical equipment with a Wenner–Schlumberger configuration. Measurements were conducted using 48 electrodes connected by four resistivity cables with an electrode spacing of 10 m, producing a survey line length of approximately 480 m. The supporting equipment included a 12 V battery, meter, and GPS (Saputra et al., 2025).



Figure 3 Multichannel Resistivity MAEX612-EM

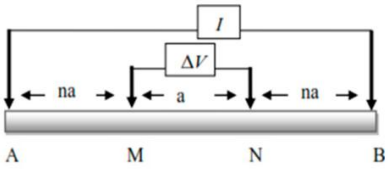


Figure 4 Wenner Schlumberger configuration

The Wenner–Schlumberger configuration uses a constant electrode spacing system where the comparison factor n represents the ratio between the distance of the current electrodes and the potential electrodes. If the distance between the potential electrodes (M–N) is a, then the distance between the current electrodes (A–B) is expressed as 2na + a (Utiya et al., 2015). Data acquisition was carried out along five transects around the Bentiring housing complex with a cable length of approximately 480 m on each line (Febriarta et al., 2019). Electrical resistivity mapping uses surface electrodes to inject electrical current into the ground while the resulting potential difference is measured by another pair of electrodes to determine subsurface resistivity variations (Crook et al., 2008).

The apparent resistivity (ρ_α) was calculated using the relationship:

$$\rho_\alpha = K \times \frac{\Delta V}{I} \quad (1)$$

Where ρ_α is the apparent resistivity (Ωm), K is the geometric factor, ΔV is the measured potential difference (V), and I is the injected current (A), for the wenner-schlumberger configuration, the geometric factor is expressed as:

$$K = \pi n(n+1)\alpha \quad (2)$$

Where a is electrode spacing and n is the spacing factor between the current and potential electrodes. Increasing electrode spacing allows deeper current penetration and greater investigation depth.

These measurements produce two-dimensional resistivity sections that represent variations in lithology and subsurface rock conditions (Comas et al., 2015; Faris et al., 2019). During data acquisition, electrode contact was ensured to minimize noise, and unstable measurements were repeated to improve data quality. Data processing was performed using Res2Dinv software through an iterative inversion process to obtain the smallest RMS error value, resulting in resistivity cross-sections that approximate actual subsurface conditions. Lithological interpretation was conducted by comparing the inversion results with reference resistivity ranges from previous studies. Weak zones were interpreted from relatively low resistivity values and discontinuities in the resistivity section that indicate subsurface heterogeneity (Pesma & Sitanggang, 2024). Materials with high water content generally exhibit lower resistivity values and weaker mechanical properties, which may represent potential weak zones in the subsurface (Amelia et al., 2024).

III. RESULT AND DISCUSSION

This study utilised primary data, employing the Wenner-Schlumberger resistivity geophysical method, which is well suited for this purpose due to its sufficient depth accuracy in detecting rock resistivity values. Based on the data processing results from the five Wenner Schlumberger configuration traverses, a resistivity cross-section model was obtained for each traverse.

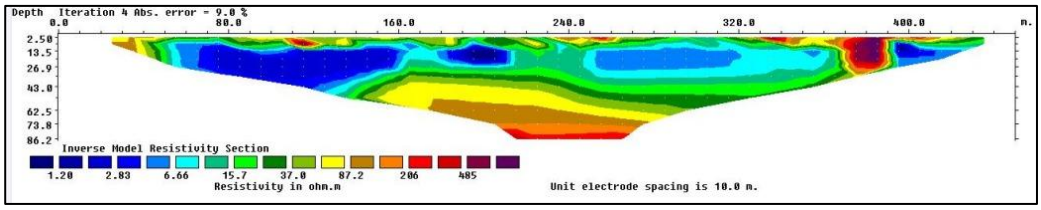


Figure 5. Results of processing data from line 1

Line 1 (Figure 5) shows the inversion results after 4 iterations with an RMS error of 9.0%, a resistivity range of 1.20–485 Ωm, and an inter-electrode spacing of 10 m. A zone of low to moderate resistivity was identified in the range of approximately 160–290 m at depths of 13.5–73.8 m. This anomaly has resistivity values of approximately 6.66–37.9 Ωm and is interpreted as clay to sandy clay material, which is relatively less consolidated compared to the higher-resistivity layers (>87.2 Ωm).

The resistivity contrast observed around the 22nd electrode (220 m) indicates lateral and vertical variations in the electrical properties of the subsurface material, reflecting changes in lithology, grain size and water content. However, this contrast merely represents differences in subsurface electrical properties and cannot be directly interpreted as evidence of deformation or subsidence without supporting data. Given the geological context of unconsolidated, fine-grained alluvial deposits, these zones of low and heterogeneous resistivity are interpreted as potential weak zones characterised by higher water saturation and lower material strength, which may affect surface stability at the study site.

Table 1 Lithology of rock type 1 (Asyari et al., 2023).

Depth (m)	Resistivity value (Ωm)	Rock type
2.50-24.9	1.03-2.35	Swamp sediment
5.3-67.5	5.29-10.3	Clay
10.3-78.8	12.3-28.2	Sandy clay
2.50-12.8	>64.7	Gravel

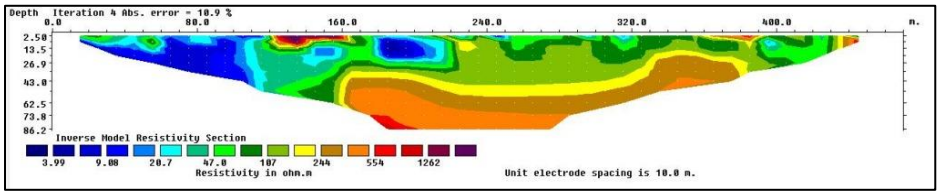


Figure 6. Results of processing data from line 2

Line 2 (Figure 6) The inversion model obtained at the 4th iteration yielded an absolute error of 10.9%, with resistivity values ranging from 3.99 to 1262 Ω·m along a 480 m survey line using 10 m electrode spacing and achieving an investigation depth of up to 86 m.. This line exhibits the highest RMS error compared to the other survey lines, which may be attributed to increased subsurface heterogeneity, stronger resistivity contrasts between materials, and the possible influence of near-surface noise or locally poor electrode contact conditions during data acquisition.

A low resistivity zone (<20 Ωm) is observed in the shallow to intermediate sections, particularly at distances of approximately 0–120 m and 150–200 m, indicating the presence of water-saturated clay and swamp-related sediments. In the central part of the line (around 160–360 m), resistivity gradually increases to >187 Ωm at depths of 30–80 m, which is interpreted as more compact materials such as sandy clay to gravel. A noticeable resistivity contrast at approximately 240–280 m reflects lateral and vertical variations in subsurface properties, representing changes in lithology, grain size, and moisture content. Based on the geological setting, these variations are interpreted as potential weak zones characterized by unconsolidated and fine-grained materials overlying more resistant layers, rather than direct evidence of deformation or subsidence.

Table 2 Lithology of rock type 2 (Asyari et al., 2023).

Depth (m)	Resistivity Value (Ωm)	Rock type
12.8-57.3	2.29-4.17	Swamp sediment
3.05-57,3	6.59-13.8	Clay
10.8-67.3	13.8-25.1	Sandy clay
12.8-78.8	>45.7	Gravel

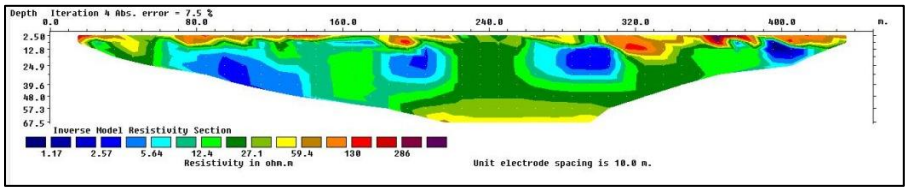


Figure 7 Results of processing data from line 3

Line 3 (Figure 6) The resistivity inversion performed up to the 4th iteration resulted in an absolute error of 7.5%, revealing subsurface resistivity values ranging from 1.17 to 286 Ω·m with 10 m electrode spacing and a maximum investigation depth of 67.5 m. A low resistivity zone (<5.64 Ω.m) developed at a distance of approximately 120-200 m and 280-360 m at a depth of 5–40 m, which was interpreted as compressible water-saturated swamp and clay sediments. Medium resistivity (12.4-59.4 Ω.m) dominates most of the cross-section and reflects clay to sandy clay, while locally occurring high resistivity (>139 Ω.m) is interpreted as coarser material such as gravel. This resistivity contrast indicates lithological heterogeneity and suggests the potential for shallow deformation zones associated with the dominance of water-saturated clay materials.

Table 3 Lithology of rock type 3 (Asyari et al., 2023).

Depth (m)	Resistivity value (Ωm)	Rock type
2.50-24.9	1.53-4.31	Swamp sediment
3.05-30.5	12.1-29.6	Clay
3-39.6	34.1-96	Sandy clay
2.50-78.8	>270	Gravel

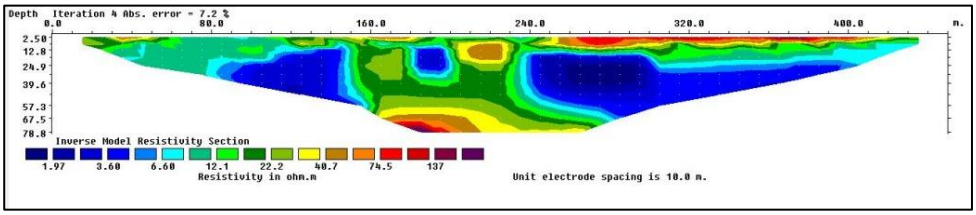


Figure 8 Results of processing data from line 4

Line 4 (Figure 8) At the 4th iteration, the inversion process achieved an absolute error of 7.2%, with interpreted resistivity values varying between 1.97 and 137 Ω·m and an investigation depth reaching up to 78.8 m using 10 m electrode spacing. The low resistivity zone (<6.60 Ωm), indicated by blue, extends quite widely at a depth of ±10–50 m, especially at a distance of about 100-180 m and 260-360 m, which is interpreted as water-saturated swamp and clay sediments. Above and around it, medium resistivity (12.1-40.7 Ω.m) develops, reflecting clay to sandy clay. Meanwhile, a higher resistivity zone (>74.5 Ω.m) appears locally in the shallow and middle sections of the cross-section, indicating coarser or more consolidated material. The dominance of low to medium resistivity layers at shallow to medium depths indicates relatively soft and compressible soil conditions, which could potentially affect surface stability along this route.

Table 4 Lithology of rock type 4 (Asyari et al., 2023).

Depth (m)	Resistivity Value (Ωm)	Rock Type
3.5-24.9	0.758-1.94	Swamp sediment
3.57-39.6	3.96-11.7	Clay
2.7-67.5	12.7-32.4	Sandy clay
5.3-78.8	>82.9	Gravel

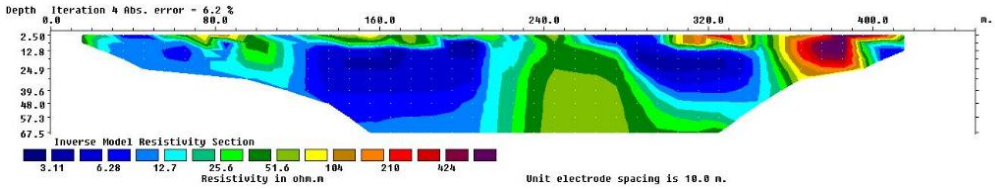


Figure 9 Results of processing data from line 5

Line 5 (Figure 9) The resistivity inversion result at the 4th iteration indicates an absolute error of 6.2%, with interpreted values varying between 3.11 and 424 Ω·m, obtained using 10 m electrode spacing and a maximum depth of investigation of 67.5 m. The low resistivity zone (<12.7 Ω.m), indicated by the blue color, extends widely in the middle of the line, especially at a distance of about 120-220 m and 280-340 m with a depth of 10-50 m, which is interpreted as water-saturated sediments in the form of clay to sandy clay. At a distance of approximately 210-310 m, there is a fairly clear resistivity contrast between the low zone and the medium resistivity zone (25.6-51.6 Ω.m), indicating lateral and vertical changes in the physical properties of the material. Meanwhile, a high resistivity zone (>210 Ω.m) appears dominant at the right end of the line at shallow depths, reflecting more compact or more consolidated material. The dominance of low resistivity layers at shallow to medium depths indicates compressible soil conditions with the potential for deformation, so that the area is interpreted as a zone prone to land subsidence.

Table 5 Lithology of rock type 5 (Asyari et al., 2023).

Depth (m)	Resistivity Value (Ωm)	Rock Type
12.8-24.9	0.600-1.47	Swamp sediment
3.05-39.6	3.59-8.78	Clay
10.8-57.3	8.78-21.5	Sandy Clay
2.50-78.8	>52.5	Gravel

Based on the results from the five survey lines, each line exhibits variations in resistivity values and anomaly depths; all reveal the presence of recurring low-resistivity zones at shallow to intermediate depths (±10–80 m), thus indicating the lateral continuity of water-saturated fine sediments in the study area. spatially, lines 1 to 5 all show low-resistivity zones that are not isolated but tend to form elongated and continuous patterns across the lines. thus, these multi-line results confirm the correlation between cross-sections, leading to the interpretation of a regional weak zone in the bentiring area, characterised by the dominance of water-saturated fine-grained material with continuous lateral distribution. this cross-track correlation approach provides a more comprehensive picture than individual interpretations, and strengthens the identification of subsurface heterogeneity zones that have the potential to be weak zones.

IV. CONCLUSION

The 2D Electrical Resistivity Imaging investigation reveals that the Bentiring residential area is underlain predominantly by water-saturated clay and sandy clay layers with low to moderate resistivity values (generally <40 Ω.m), indicating weak and compressible subsurface conditions. These mechanically weak strata consistently appear at shallow to intermediate depths across all five lines and are laterally associated with resistivity contrasts that suggest structural discontinuities and localized deformation zones. The most prominent weak zone is clearly delineated on Line 1, while similar low-resistivity anomalies on Lines 2-5 indicate areas susceptible to ground instability and potential subsidence. The results confirm that subsurface heterogeneity, controlled by saturated fine-grained alluvial deposits, plays a significant role in reducing bearing capacity in the study area. Scientifically, this study demonstrates the effectiveness of ERI in delineating mechanically vulnerable layers in urban environments. Practically, the presence of shallow compressible clay and sandy clay units highlights the need for detailed geotechnical assessment, controlled groundwater management, and soil improvement measures prior to further infrastructure development to mitigate future land subsidence hazards.

ACKNOWLEDGEMENTS

The author would like to thank the Physics Laboratory of Bengkulu University for providing a set of equipment (Multichannel Resistivity Meter MAE X612-EM) and Res2dinv software.

CONFLICT OF INTEREST

The authors declare no conflict of interest.

FUNDING STATEMENT

This research received no specific funding.

DECLARATION OF GENERATIVE AI AND AI-ASSISTED TECNOLOGIES IN THE WRITING PROCESS

GPT was used solely to correct grammatical and typographical errors. The author bears full responsibility for the content and integrity of the publication.

REFERENCES

Adenika, C. I., Ariyibi, E. A., Awoyemi, M. O., Adebayo, A. S., Dasho, O. A., & Olagunju, E. O. (2018). Application of Geophysical Approach to Highway Pavement Failure : A Case Study From Basement Complex Terrain Southwestern Nigeria. *International Journal of Geo-Engineering*, *9*(8), 1–22. https://doi.org/10.1186/s40703-018-0076-0

Amelia, D., Widyaningrum, Y., & Indriawati, A. (2024). Identifikasi Zona Lemah Tanggul Daerah Aliran Sungai (DAS) Bumang Desa Kemuja Menggunakan Metode Geolistrik Resistivitas Konfigurasi Wenner. *Jurnal Riset Fisika Indonesia*, *5*(1), 29–37.

Asyari, T. D., Sailah, S., Kaban, H., & Jorena. (2023). Identifikasi Litologi Batuan Menggunakan Metode Geolistrik Sebagai Penyelidikan Awal Pembangunan Turap di Tepi Sungai. *Jurnal Penelitian Sains*, *25*(3), 279–282.

Comas, X., Terry, N., Slater, L., Warren, M., Kolka, R., Kristiyono, A., Sudiana, N., Nurjaman, D., & Darusman, T. (2015). Imaging Tropical Peatlands in Indonesia Using Ground-Penetrating Radar (GPR) and Electrical Resistivity Imaging (ERI): Implications for Carbon Stock Estimates and Peat Soil Characterization. *Biogeosciences*, *12*(10), 2995–3007. https://doi.org/10.5194/bg-12-2995-2015

Crook, N., Binley, A., Knight, R., Robinson, D. A., Zarnetske, J., & Haggerty, R. (2008). Electrical Resistivity Imaging of the Architecture of Substream Sediments. *Water Resources Research*, *44*(W00D13), 1–11. https://doi.org/10.1029/2008WR006968

Faris, A. N., Suaidi, D. A., Sutrisno, Hasan, M. F. R., & Broto, A. B. (2019). Identifikasi Sebaran Akuifer dengan Metode Geolistrik Resistivitas Konfigurasi Schlumberger di Desa Gedangan, Kecamatan Gedangan, Kabupaten Malang. *NATURAL B*, *5*(1), 28–34.

Fatoni, A. R., Supriyanto, & Lazar, P. A. (2021). Identifikasi Zona Lemah Di Jalan Poros Samarinda Bontang Dengan Menggunakan Metode Geolistrik Konfigurasi Wenner Schlumberger. *Jurnal Geosains Kutai Basin*, *4*(1), 1–7.

Febriarta, E., Suswanti, & Noviandaru, S. (2019). Interpretasi Electrical Resistivity Tomography (ERT) Untuk Pendugaan Air Tanah Dangkal Pada Formasi GunungApi Muda. *Jurnal Nasional Teknologi Terapan*, *3*(1), 49–62.

Gafoer, S., Amin, T. C., & Pardede, R. (2007). Peta Geologi Lembar Bengkulu, Sumatera (Skala 1:250.000). Pusat Penelitian dan Pengembangan Geologi, Bandung

Lubis, A. M., Butarbutar, D. C., Suhendra, & Samdara, R. (2019). Investigasi Sudut Pergerakan Sesar Di Segmen Musi Kepahiang dengan Menggunakan Metode Geolistrik. *Jurnal Meteorologi Dan Geofisika*, *20*(2), 67–72.

Lutfinur, I., Khumaedi, & Susanto, H. (2015). Identifikasi Sesar Bawah Permukaan Menggunakan Metode Geolistrik Konfigurasi Schlumberger (Studi Kasus Sungai Opak Yogyakarta). *Indonesian Journal of Applied Physics*, *5*(2), 10–24.

Makmur, S., Sehah, & Sugito. (2016). Analisis Zona Lemah (Amblesan) Di Kawasan Jalan Raya Gunung Tugel Kabupaten Banyumas Berdasarkan Survei Geolistrik Konfigurasi Wenner. *Techno*, *17*(2), 111–121.

Manuho, J., As'ari, & Pasau, G. (2015). Identifikasi Patahan Manado Dengan Menggunakan Metode Geolistrik Konfigurasi Half Schlumberger Di Kota Manado. *Jurnal Ilmiah Sains*, *15*(1), 16–19.

Nuraini, F. (2023). *Identifikasi Struktur Bawah Permukaan Di Perumahan Bentiring Permai 3, Kota Bengkulu Berdasarkan Metode VES*.

Paembonan, A. Y., Febriansanu, D. R., Sinaga, R. E., Putra, F. D., & Rahmanda, V. (2020). Investigasi Air Tanah Pada Endapan Piroklastik dengan Menggunakan Metode Electrical Resistivity Imaging (ERI). *Gravitasi*, *19*(1), 1–5.

Pesma, R. A., & Sitanggang, A. F. (2024). Pendugaan Zona Sesar Berdasarkan Geolistrik 2D Pada Ulujadi, Kota Palu, Sulawesi Tengah. *Jurnal Geofisika Eksplorasi*, *10*(01), 5–15.

Rizqi, A. H. F., Yudhana, W. M. B., Uligawati, G. W., & Basri, R. R. (2020). Penyelidikan Geolistrik Menggunakan Konfigurasi Schlumberger Terhadap Potensi Amblesan Daerah Ponjong, Gunung Kidul. *KURVATEK*, *5*(2), 31–40.

Saputra, B., Suhendra, Halauddin, & Lidiawati, L. (2025). Identification of Areas at Risk of Abrasion Application of Electrical Resistivity Tomography (ERT) Method on Nangai Beach, North Bengkulu. *Jurnal Fisika Dan Aplikasinya*, *21*(3), 87–91.

Sugianto, N., Farid, M., & Suryanto, W. (2016). Local Geology Condition Of Bengkulu City Based On Seismic Vulnerability Index (Kg). *ARPN Journal of Engineering and Applied Sciences*, *11*(7), 4797–4803.

Utiya, J., As'ari, & Tongkukut, S. H. (2015). Metode Geolistrik Restivitas Konfigurasi Wenner-Schlumberger dan Konfigurasi Dipole-Dipole Untuk Identifikasi Patahan Manado di Kecamatan Paaldua Kota Manado. *Jurnal Ilmiah Sains*, *15*(2), 135–141.

Wulandari, W., Manrulu, R. H., & Jusmi, F. (2024). Identifikasi Zona Lemah Daerah Longsor Desa Maliwowo Menggunakan Metode Geolistrik Konfigurasi Wenner-Schlumberger. *Applied Physics of Cokroaminoto Palopo*, *6*(1), 7–12.